J Mater Sci (2008) 43:1492–1496
DOI 10.1007/s10853-007-2274-6

Fabrication of nanosized metallic copper by electrochemical milling process

Da-Wei Zhang · Chun-Hua Chen · Jin Zhang · Fei Ren

Received: 24 June 2007 / Accepted: 29 October 2007 / Published online: 12 December 2007

Abstract Using a copper oxide powder of micrometer size as the starting electrode material in CuO/Li cells, copper oxide (CuO) can be electrochemically reduced into metal particles of smaller sizes in a controllable way. A novel electrochemical milling (ECM) method is developed for a "top–down" synthesis of nanometer-scaled metal particles. X-ray diffraction (XRD), field-emission scanning electron microscopy (FESEM), and transmission electron microscopy (TEM) were employed to characterize the structure of copper particles obtained by the electrochemical reduction. The influences of CuO precursors, current density, and operating temperature on the final products were also studied. It is found that the latter two factors had pronounced effects on the obtained copper products.

Introduction

Nanosized metal materials have attracted much technological and scientific attention due to their interesting physical and chemical properties, which should accelerate their extensive applications in the nanodevices [1–4]. Among all the metals copper is the most commonly used one, because nanosized copper has some advantages over other metals in common uses such as lower resistance, higher allowed current density and increased scalability [5]. Thus, a number of ways have been tried to synthesize nanosized metallic copper, including template synthesis [6–9], electrochemical deposition [10–13], reduction of copper compounds in solution [14–17], and other novel methods [18, 19]. By these methods, nanosized copper with uniform and controllable dimensions could be obtained, but the complicated synthesis process, the requirements for special instruments or harsh conditions and the usually low-yield limit their applications in practice.

In our recent work on the lithium ion battery a novel electrochemical milling (ECM) process was developed to fabricate nanosized copper spheres and fibers. It is widely acknowledged that copper oxide (CuO) may be used as a new class of electrode materials for rechargeable lithium–ion batteries [20–23]. During the discharge step, the CuO electrode is converted into metallic copper grains dispersed in a Li_2O matrix [21, 22]. Thus, in our previous research work on the lithium ion battery, CuO/Li cells were used as "micro-reactor" to synthesize copper particles by discharging CuO electrode [24]. Yu et al. further studied the ECM process on other transition metal oxides by using their thin-film type electrodes as the starting materials [25]. Maier' group also applied the same strategy on the synthesis of nanosized Pt from Li cells [26]. In this article we present the effects of a few control parameters such as temperature and CuO precursors on the size and morphology of the final products, in order to develop a controllable synthesis approach.

Experimental section

All the metallic copper particles were fabricated in electrochemical cells with CuO electrode versus Li counter

D.-W. Zhang
Department of Chemical Engineering and Technology, Hefei University of Technology, Hefei, Anhui 230009, P.R. China

D.-W. Zhang (✉) · C.-H. Chen · J. Zhang · F. Ren
Department of Materials Science and Engineering, University of Science and Technology of China, Hefei, Anhui 230026 P.R. China
e-mail: zhangdw@ustc.edu.cn

electrode. The used coin cells (CR2032) of the Li | 1 M LiPF6 (EC:DEC = 1:1) | CuO were assembled in an Ar-filled glove box (MBraun Labmaster 130), where EC and DEC, respectively, stand for ethylene carbonate and diethyl carbonate. The CuO electrode was prepared by casting a slurry consisting of 90 wt.% CuO and 10 wt.% poly (vinylidene fluoride) (PVDF) onto a copper foil. Here, PVDF served as the binder with a wide stable electrochemical window. The cells were discharged to 0 V on a multi-channel battery test system (NEWARE BTS-610). After the discharge, the cells were disassembled in the Ar-filled glove box. Then the CuO electrode films were washed with pure DEC to remove the electrolyte residue before they transferred outside of the glove box. They were further washed with 1-methyl-2-pyrrolidone (NMP), a dilute hydrochloric acid and anhydrous ethanol to remove PVDF, Li_2O and the residual copper oxide. The resulting solid product was finally separated in a centrifuge machine (15,000 rpm). The obtained powder was brought for characterization by X-ray diffraction (Philips X'Pert Pro Super, CuK_α radiation) and transmission electron microscopy (Hitachi 800). Lithium contents of the discharged electrode film and the powders obtained finally were determined by inductively coupled plasma-atomic emission spectrometer (ICP-AES, Atomscan Advantage, USA).

Results and discussion

The initial discharge experiment

The initial discharge experiment was conducted under a set of fixed conditions. The CuO powders used as the electrode were of analytical grade and were composed of micrometer scaled CuO particles. The cells were discharged at room temperature with the discharge current of 0.064 mA/cm^2. After discharged and washed, the final powder product was obtained and transferred to the sample chamber of an X-ray diffractometer without exposure in air. This discharge experiment has been discussed in our previous paper [24]. The X-ray diffraction (XRD) pattern of the final products is shown in Fig. 1. Obviously, only copper is left after the washing procedure. The rather sharp diffraction peaks suggest a high crystallinity of these copper particles with an average crystallite size of 35 nm, which is calculated with the Scherrer equation. The lattice parameter (a) of a unit cell is estimated to be 0.361 nm, which is very close to the reported data (JCPDS 4-836 $a = 3.615$ Å). From this pattern it can be seen that reaction (1) was easily accomplished in the "micro-reactor" and this ECM process is feasible to obtain metallic copper.

$$CuO + 2Li \rightarrow Cu + Li_2O \quad (1)$$

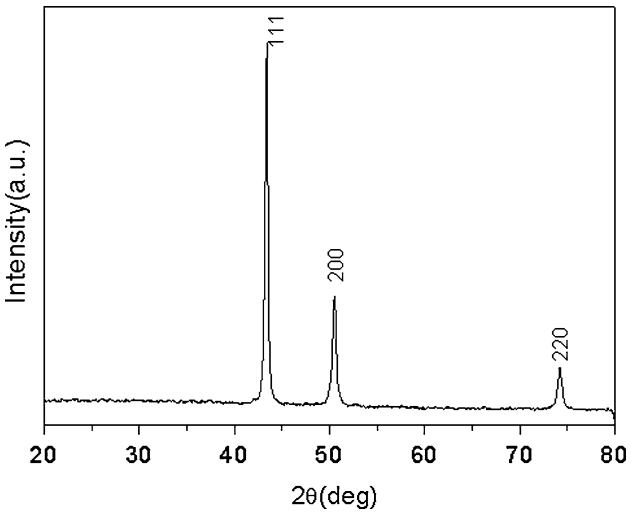

Fig. 1 The XRD patterns of the Cu powders recovered from the electrochemical reduction process

According to the test of ICP-AES, after fully discharged lithium content is 10.4% in the electrode film, which quantificationally describes the lithium insertion into CuO electrode in reaction (1). The lithium content of the powders obtained finally is 0%, which shows Li_2O was cleared away after washing the electrode film with dilute hydrochloric acid and anhydrous ethanol.

The size and morphology of the precursor CuO powder and the obtained copper particles are shown by their scanning electron micrographs (Fig. 2). Thus, in these Li cells the CuO electrodes are composed of commercial CuO powders with a particle size of about 4 μm (Fig. 2a). After the ECM process a large scale of nano-sized copper has been fabricated as shown in Fig. 2b. The size of the nanoparticles is about 40 nm, being consistent with the calculated XRD result based on Scherrer equation. Hence,

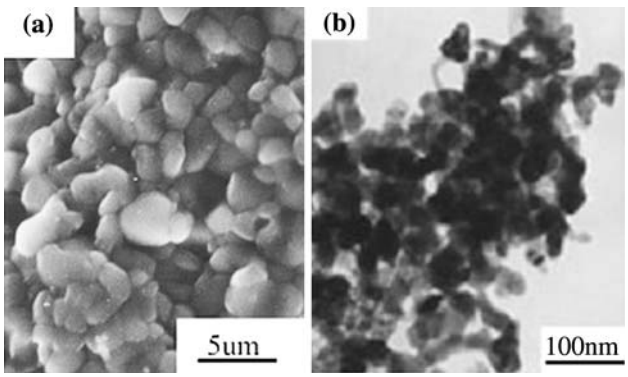

Fig. 2 The scanning electron micrographs of the starting CuO powder (**a**), and the TEM image of the discharged products (metallic copper) obtained at the current density of 0.064 mA/cm^2 in room temperature (**b**)

after the electrochemical reduction process the micrometer-sized CuO particles are milled into nanosized copper particles.

According to Burbank's work on lead acid batteries [27], a metasomatic transformation mechanism is adopted to explain the Li-driven transformation when Li is electrochemically inserted into metal oxide. In this mechanism, the global particle shape is retained after driving metal atoms out of the metal oxide precursor, but more elementary particles (e.g., nanograins) of different shape and size from the precursor are produced. Specifically, when CuO electrode is reduced in a Li cell the reaction (2) occurs initially and the intermediate product Cu_2O is formed [16, 28]. Since Cu_2O and final products (Li_2O) respectively have a cubic-type structure with $\alpha = 4.267$ Å and 4.614 Å, one can easily imagine that when the reaction (3) occurs, Li will enter into the oxygen framework in Cu_2O and the copper is pushed out of the lattice, forming elemental copper. Then the copper nucleation and growth process lead the formation of copper nanoparticles.

$$CuO + Li \rightarrow \frac{1}{2}Cu_2O + \frac{1}{2}Li_2O \quad (2)$$

$$\frac{1}{2}Cu_2O + Li \rightarrow Cu + \frac{1}{2}Li_2O \quad (3)$$

Effects of CuO precursor on final product

In our previous research work, another CuO sample composed of nanosheet particles (Fig. 3a) was used to make CuO/Li cells in order to analyze its electrochemical properties [29]. To investigate the influence of precursor CuO on final product, the final electrochemically milled product of this CuO sample was also characterized to compare with the previous CuO electrode. The transmission electron microscopy (TEM) analysis (Fig. 3b) demonstrates that the final product also consists of a large quantity of nanoparticles with a uniform diameter of about 40 nm, which is similar to the electrochemical reduction products obtained from previous CuO electrode. This result illuminates that the morphology and size of the CuO precursor have little influence on the final reduction products.

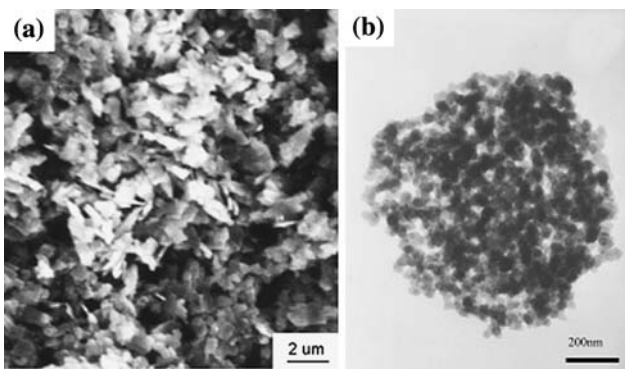

Fig. 3 The scanning electron micrographs of the CuO powder shaped in nanosheet (**a**), and the TEM image of the discharged products (metallic copper) obtained at the current density of 0.064 mA/cm^2 at room temperature (**b**)

It is easy to interpret this result according to the metasomatic transformation mechanism. Since when Li enters into the oxygen framework of the intermediate product Cu_2O, copper atoms are pushed out and then the morphology and size of the precursor CuO have already had nothing to do with the copper nucleation and growth process. Thus, when the external conditions are definite, the morphology and size of the precursor CuO have no effect on the final products.

Effects of discharge current on the nanograins growth

When the Li cells are discharged, different current density are adopted to analyze the effects on the copper nanograins growth. Figure 4 shows the TEM images of the samples after discharged with different current densities, such as 0.32 mA/cm^2 and 0.032 mA/cm^2. Compared with the results of 0.064 mA/cm^2 in the initial experiment (Fig. 2b), when at a larger current density of 0.32 mA/cm^2, a large quantity of uniform and spherical nanoparticles are obtained, but with a larger size of 100 nm (Fig. 4a). When the current density is decreased to 0.032 mA/cm^2, "octopus"-shaped copper particles are obtained in the final product (Fig. 4b). Field-emission scanning electron microscopy (FESEM) images shows this surprising "octopus" structure consists of many nanofibers with a rather uniform thickness of about 40 nm originated from a core (Fig. 4c).

Obviously, the current density has a pronounced influence on the morphology and size of the nanosized copper products. Since there is no electronic conducting additive (carbon black) in the CuO electrode composition, the electronic conduction on the CuO electrode controls the growth of the copper particles. As showed in reaction (2) and (3), Cu and Li_2O are finally formed when lithium inserted into the CuO electrode. In this process the electronic conduction should be the copper particles growing along the Li_2O matrix, since Li_2O is insulating. Obviously, the electronic conductivity is proportional to the size of the copper particles. So, as showed in Fig. 4a and b, in a larger current density (0.32 mA/cm^2) the obtained Cu particles are larger than in a smaller current density (0.064 mA/cm^2) so as to maintain a fast reduction process. However this order is broken in a very small current density (0.032 mA/cm^2), in which copper can only be pushed out of the Li_2O structure by forming many nanofibers emanating from a core

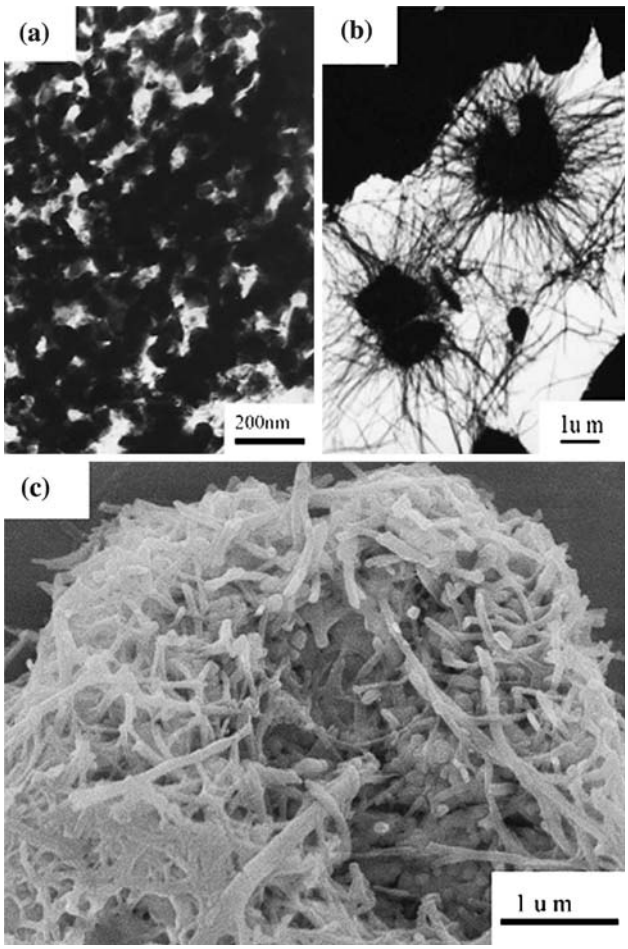

Fig. 4 The TEM images of the discharged products (metallic copper) obtained at different current density of 0.32 mA/cm^2 (**a**), 0.032 mA/cm^2 (**b**) in room temperature; The FESEM image of the discharged products (metallic copper) obtained at the current density of 0.032 mA/cm^2 in room temperature (**c**)

(Fig. 4c). This result is similar as the copper dendrimers growing on the discharged product of $Cu_{2.33}V_4O_{11}$ [30]. Basically, the electron conduction involved in the reaction (1) follows the path with the least resistance. At a small current density, the reduction takes place first at some (but not all) contact points between the CuO and the current collector. As long as some copper grains are produced at these points, the electrons would preferentially pass through them and thus lead to the formation of copper fibers. Microscopically, this process can be realized by pushing copper out of the original CuO particles and form a similar dendritic structure as in $Cu_{2.33}V_4O_{11}$. On the other hand, at a large current density, the copper may be formed at all the contact points between CuO particles and the current collectors, and no orientational growth or dendrimer formation is necessary. Hence, spherical copper particles are obtained at a large current density.

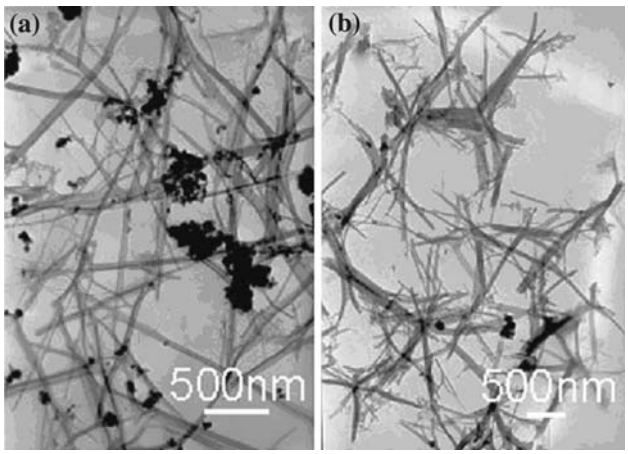

Fig. 5 The TEM images of the discharged products (metallic copper) obtained at different temperatures of 70 °C (**a**), 0 °C (**b**) at the current density of 0.032 mA/cm^2

Influences of the temperature

Since temperature can influence the rate of conversion reaction (1) or the rate of generating copper, we also discharged the assembled cells at different temperatures of 0 °C, and 70 °C at a small current density of 0.032 mA/cm^2 to compare the results with that obtained at room temperature (Fig. 4b). As shown in Fig. 5a, when discharged at 70 °C copper nanofibers are also formed, but the product also comprises large numbers of spherical nanoparticles. The diameter of the obtained copper nanofibers and nanoparticles is about 40–50 nm. At the same time when discharged at 0 °C the copper product are all nanofibers (Fig. 5b) with the width of about 50 nm, which is similar to the product obtained at room temperature. This means that the temperature for discharging can influence the morphology of reduction-derived copper particles.

As discussed above, in the case of the nanofibers obtained by a room temperature discharging with a small current density of 0.032 mA/cm^2, the least resistance path for the electron conduction is along the copper nanofibers. When discharged at 0 °C, the rate of the reduction reaction (1) is even slower than at room temperature, which results in more orientational growth of copper nanofibers (Fig. 5b). However, when discharged at 70 °C the reaction (1) proceeds faster, resulting in the decrease of the degree of orientational growth. Consequently, the formation of both copper nanofibers and spherical particles is observed (Fig. 5a).

Conclusions

In this article, the CuO/Li cells are used as "micro-reactor" to fabricate nanosized metallic copper by electrochemically reducing CuO electrode. This novel way can be described

as an ECM process. The formation mechanism of copper nanoparticles can be interpreted with a metasomatic transformation process. The most important factors to influence the structure of the generated copper products are the current density and operating temperature. The morphology of the CuO precursors is found to have a little effect on the final copper products. We believe that such an ECM process is versatile and could be adapted for the fabrication of 1D nanostructures of various transition metals by choosing the suitable discharge conditions.

Acknowledgements This study was supported by National Science Foundation of China (Grant No. 20703013 and 20471057). We are also grateful to The Ministry of Education (SRFDP No. 2003035057) and the PD Foundation of China (Grant No. 20070410218).

References

1. Zhang Z, Sun X, Dresselhaus MS, Ying JY (2000) Phys Rev B 61:4850
2. Wang ZL (2000) Adv Mater 12:1295
3. Sun L, Searson PC, Chien CL (2001) Appl Phys Lett 79:4429
4. Cui Y, Wei Q, Park H, Lieber CM (2001) Science 293:1298
5. Monson CF, Woolley AT (2003) Nano Lett 3:359
6. Yen MY, Chiu CW, Hsia CH, Chen FR, Kai JJ, Lee CY, Chiu HT (2003) Adv Mater 15:235
7. Tanori J, Pileni MP (1997) Langmuir 13:639
8. Ziegler KJ, Harrington PA, Ryan KM, Crowley T, Holmes JD, Morris MA (2003) J Phys: Condens Mat 15:8303
9. Wang JW, Li YD (2003) Adv Mater 15:445
10. Motoyama M, Fukunaka Y, Sakka T, Ogata YH, Kikuchi S (2005) J Electroanal Chem 584:84
11. Gao T, Meng GW, Wang YW, Sun SH, Zhang LD (2002) J Phys: Condens Mat 14:355
12. Zhang MZ, Wang Y, Yu GW, Wang M, Peng RW, Weng YY, Ming NB (2004) J Phys: Condens Mat 16:695
13. Molares MET, Buschmann V, Dobrev D, Neumann R, Scholz R, Schuchert IU, Vetter J (2001) Adv Mater 13:62
14. Lisiecki I, Filankembo A, Sack-Kongeh H, Eeiss K, Pileni MP, Urban J (2000) Phys Rev B 61:4968
15. Liu ZP, Yang Y, Liang JB, Hu ZK, Li S, Peng S, Qian YT (2003) J Phys Chem B 107:12658
16. Chang YH, Wang HW, Chiu CW, Cheng DS, Yen MY, Chiu HT (2002) Chem Mater 14:4334
17. Han WK, Choi JW, Hwang GH, Hong SJ, Lee JS, Kang SG (2006) Appl Surf Sci 252:2832
18. Li CM, Lei H, Tang YJ, Luo JS, Liu W, Chen ZM (2004) Nanotechnology 15:1866
19. Wang PI, Zhao YP, Wang GC, Lu TM (2004) Nanotechnology 15:218
20. Poizot P, Laruelle S, Grugeon S, Dupont L, Tarascon JM (2000) Nature 407:496
21. Grugeon S, Laruelle S, Urbina HR, Dupont L, Poizot P, Tarascon JM (2001) J Electrochem Soc 148:A285
22. Debart A, Dupont L, Poizot P, Leriche JB, Tarascon JM (2001) J Electrochem Soc 148:A1266
23. Gao XP, Bao JL, Pan GL, Zhu HY, Huang PX, Wu F, Song DY (2004) J Phys Chem B 108:5547
24. Zhang DW, Chen CH, Zhang J, Ren F (2005) Chem Mater 17:5242
25. Yu Y, Chen CH, Shui JL, Xie S (2005) Angew Chem Int Ed 44:7085
26. Hu YS, Guo YG, Sigle W, Hore S, Balaya P, Maier J (2006) Nat Mater 5: 713
27. Burbank J (1966) J Electrochem Soc 113:10
28. Novak P (1985) Electrochim Acta 30: 1687
29. Zhang DW, Yi TH, Chen CH (2005) Nanotechnology 16:2338
30. Morcrette M, Rozier P, Dupont L, Mugnier E, Sannier L, Galy J, Tarascon JM (2003) Nat Mater 2:755